RERTR 2009 - 31st INTERNATIONAL MEETING ON REDUCED ENRICHMENT FOR RESEARCH AND TEST REACTORS

November 1-5, 2009
Kempinski Hotel Beijing Lufthansa Center
Beijing, China

INTERDIFFUSION IN DIFFUSION COUPLES: U-MO VS. Al and Al-Si

E. Perez, B. Yao, Y.H. Sohn
University of Central Florida, Orlando, FL, 32816, USA

and

D.D. Keiser, Jr.
Idaho National Laboratory, Idaho Falls, ID, 83403, USA

ABSTRACT

Interdiffusion and microstructural development in the U-Mo-Al system was examined using solid-to-solid diffusion couples consisting of U-7wt.%Mo, U-10wt.%Mo and U-12wt.%Mo vs. pure Al, annealed at 600°C for 24 hours. The influence of Si alloying addition (up to 5 wt.%) in Al on the interdiffusion microstructural development was also examined using solid-to-solid diffusion couples consisting of U-7wt.%Mo, U-10wt.%Mo and U-12wt.%Mo vs. pure Al, Al-2wt.%Si, and Al-5wt.%Si annealed at 550°C up to 20 hours. Scanning electron microscopy (SEM), transmission electron microscopy (TEM) and electron probe microanalysis (EPMA) were employed to examine the development of a very fine multi-phase intermetallic layer. In ternary U-Mo-Al diffusion couples annealed at 600°C for 24 hours, interdiffusion microstructure varied of finely dispersed UAl_3, UAl_4, $U_6Mo_4Al_{43}$, and UMo_2Al_{20} phases while the average composition throughout the interdiffusion zone remained constant at approximately 80 at.% Al. Interdiffusion microstructure observed by SEM/TEM analyses and diffusion paths drawn from concentration profiles determined by EPMA appear to deviate from the assumption of "local thermodynamic equilibrium," and suggest that interdiffusion occurs via supersaturated UAl_4 followed by equilibrium transformation into UAl_3, $U_6Mo_4Al_{43}$, UAl_4 and UMo_2Al_{20} phases. Similar observation was made for U-Mo vs. Al diffusion couples annealed at 550°C. The addition of Si (up to 5 wt.%) in Al significantly reduced the thickness of the intermetallic layer by changing the constituent phases of the interdiffusion zone developed in U-Mo vs. Al-Si diffusion couples. Specifically, the formation of $(U,Mo)(Al,Si)_3$, with relatively large solubility for Mo and Si, and UMo_2Al_{20} phases was observed along with disappearance of $U_6Mo_4Al_{43}$ and UAl_4 phases. Simplified understanding based on U-Al, U-Si, and Mo-Si binary phase diagrams is discussed in the light of the beneficial effect of Si alloying addition.

1. Introduction

U-Mo (7~12 wt.% Mo) alloys as dispersed and monolithic fuel extruded within Al-alloys, are being developed as a low enriched metallic fuel for the Reduced Enrichment for Research Test Reactor (RERTR) program [1,2,3]. The U-Mo alloys have a great potential as the metallic fuel due to their high uranium density and phase stability [4-11]. However, interactions via interdiffusion [7,8] between U-Mo and Al-alloys have been observed, during both processing and irradiation, and can adversely affect the fuel performance [5,12-18]. The interdiffusion zone (IDZ) in general consists of a complex, multi-phase layer that can rapidly grow and deteriorate the performance of the fuel system. [4-48]. Thus, improved performance and service life of U-Mo dispersion and monolithic fuels warrant a clearer understanding of the phase constituents and growth of the interaction layer (i.e., IDZ) that develops between the U-Mo and Al alloys.

In this study, the phase constituents and growth of the interaction layers that develop between U-Mo alloys and Al-alloys were examined using solid-to-solid diffusion couples assembled using U-7Mo, U-10Mo and U-12Mo (wt.%) vs. pure Al, Al-2Si and Al-5Si (wt.%) alloys. A series of diffusion couples were annealed at 550°C and 600°C for various periods up to 24 hours. Phase constituents, thickness and concentration profiles were examined by using X-ray diffraction (XRD), scanning electron microscopy (SEM), electron probe microanalysis (EPMA) and transmission electron microscopy (TEM).

2. Procedure

To prevent oxidation of U-Mo and Al-alloys, they were continuously handled and metallographically prepared under an Ar atmosphere in a glove box. The U-Mo alloys were cast using high purity depleted U (DU) and Mo via triple arc melting, and drop cast to form rods with 6.35 mm diameter. The as-cast rods were homogenized at 950°C for 48 hours and water-quenched. All U-Mo alloys consisted of bcc γ-phase prior to diffusion anneal, and their compositions were verified by EPMA with pure elemental standards. The Al-Si alloys were prepared with high purity Al and Si using similar triple arc melting at Ames National Laboratory, Ames, Iowa. High purity Al rods were purchased from a commercial source.

U-Mo and Al-alloy rods were sectioned into disks, 6.35 mm in diameter and 2-4 mm in thickness. The faces of discs were metallographically polished down to 1 μm using diamond paste. The Al-alloys were then treated with concentrated HNO_3 to improve bonding by dissolving any remaining trace of oxides that may have been present on polished surfaces. The polished discs were then placed in contact with each other, and held together by two clamping discs with stainless steel rods to form a jig. The jig assembly was then encapsulated in quartz capsule and sealed under an Ar atmosphere after repeated vacuum (10^{-6} torr) and H_2 purge. Ta foil was placed inside the capsules prior to sealing to serve as an oxygen trap. All couples were annealed using a Lindberg/Blue™ three-zone tube furnace. After annealing, the diffusion couples were quenched by breaking the quartz capsule in ice water. Each diffusion couple was then mounted in epoxy, cross-sectioned and polished down to 1 μm using diamond paste for compositional and microstructural examination.

Phase constituents, thickness and concentration profiles were examined by using scanning electron microscopy (SEM), electron probe microanalysis (EPMA) and transmission electron microscopy (TEM). Backscatter electron imaging and X-ray energy dispersive spectroscopy (XEDS) were initially employed to observe the thickness, phase constituents and microstructure of the interaction layer. Based

on SEM/XEDS analyses, selected areas within the IDZ were prepared for TEM analysis. In this paper, we highlight the TEM results obtained for diffusion couples, U-10Mo vs. Al annealed at 600°C for 24 hours and U-7Mo vs. Al-5Si annealed at 550°C for 5 hours. TEM specimens were prepared by using a focus ion beam (FIB) in-situ lift-out (INLO) technique. A FEI/TecnaiTM F30 300keV TEM equipped with a Fischione™ high angle annular dark field (HAADF) detector and EDXS™ (XEDS) was employed for TEM analysis. Selected area electron diffraction (SAED) and convergent beam electron diffraction (CBED) patterns from various phases were collected and indexed using the Digital Micrograph™ analysis software.

3. Results

3.1 Diffusion Couples U-Mo vs. Pure Al

Figure 1 presents backscatter electron micrographs of (a) U-7Mo vs. Al, (b) U-10Mo vs. Al and (c) U-12Mo vs. Al diffusion couples annealed at 600°C for 24 hours. On these micrographs, dark regions on top correspond to Al and the light-gray regions on the bottom correspond to U-Mo alloys. The interaction layer that developed due to interdiffusion appears dark-gray. Development of interaction layer is consistent throughout the cross-section of the specimens. Table I reports the measured thickness of the IDZ, T, along with the growth constant, K, define by $T= K*t^{1/2}$, where t is the anneal time. This growth constant, simply assumes the development of IDZ to be purely parabolic. The growth constant varied as a function of Mo content in the U-Mo alloy between 0.9 and 1.84 $\mu m/sec^{1/2}$ with the maximum value observed for U-10Mo alloy.

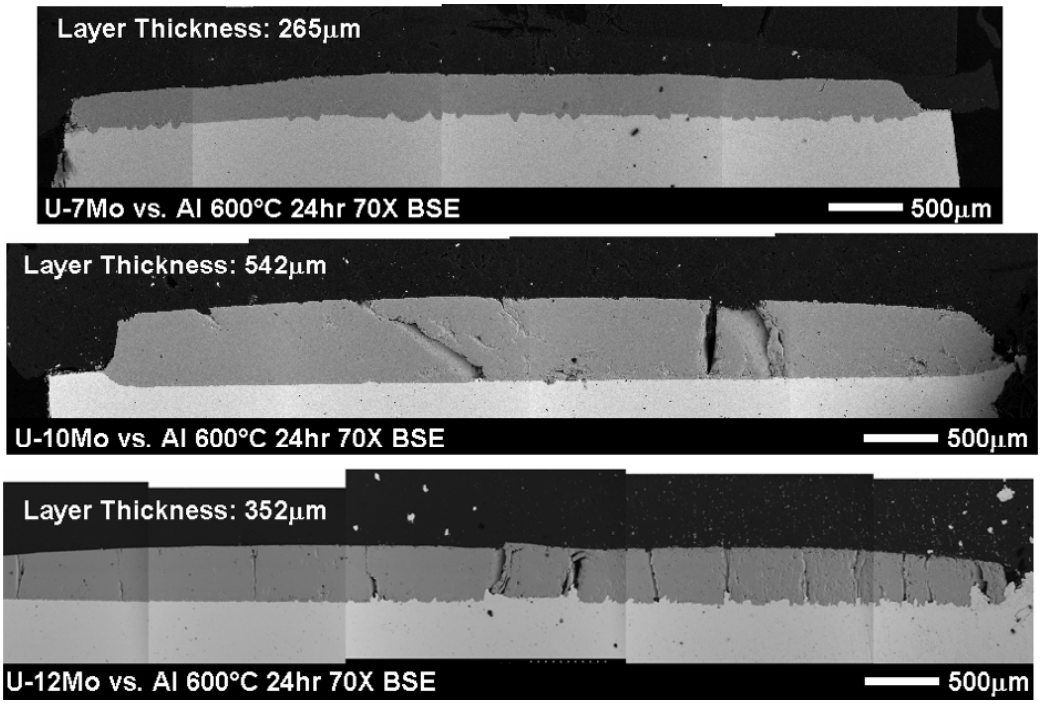

Figure 1. Backscatter electron micrographs of (a) U-7Mo vs. Al, (b) U-10Mo vs. Al and (c) U-12Mo vs. Al diffusion couples annealed at 600°C for 24 hours.

Table I. Thickness and diffusion-controlled growth constant for interaction layer in diffusion couples, U-Mo vs. Al, annealed at 600C for 24 hours.

Diffusion Couple	Average Thickness (μm)	Growth Constant, K (μm/sec$^{1/2}$)
U-7Mo vs. Al	265	0.90
U-10Mo vs. Al	542	1.84
U-12Mo vs. Al	352	1.20

Figure 2 presents typical EPMA concentration profiles obtained from diffusion couple U-10Mo vs. Al annealed at 600°C for 24 hours. The U-7Mo vs. Al and U-12Mo vs. Al couples exhibited similar concentration profiles with negligible gradients of concentration. Only a slight difference in U-Mo concentrations, based on U-Mo alloy composition, was observed while Al concentration remained approximately at 80 at.% regardless of Mo content. The high Al content suggests the presence of aluminides in the interaction layers. Only very small gradients in the concentration profiles, up to 2 at.%, were observed across the thickness of the IDZs. Although measured changes in concentrations are repeatable, these changes in concentration are within experimental uncertainty, and could not be analyzed further in terms of concentration gradients.

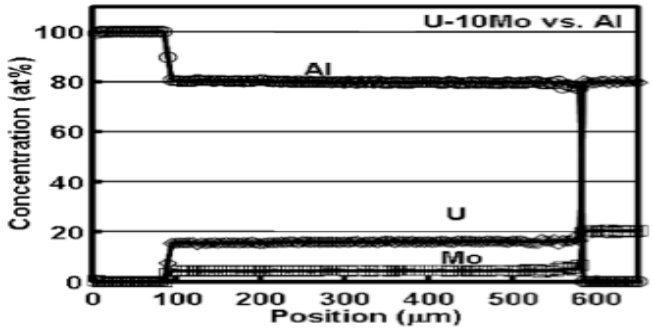

Figure 2. Concentration profiles obtained by EPMA for diffusion couples U-10Mo vs. Al annealed at 600°C for 24 hours. The U-7Mo vs. Al and U-12Mo vs. Al exhibits similar concentration profiles with slight difference in U-Mo concentrations based on Mo content within the U-Mo alloys.

The IDZs between the U-Mo and Al developed a stratified microstructure that consisted of fine-scaled multi-phase regions. The strata were defined by observable microstructural changes in the IDZs. All diffusion couples contained a central stratum that constituted the majority of their thickness. A typical backscatter electron micrograph of the IDZ in U-7Mo vs. Al diffusion couple annealed at 600°C for 24 hours is presented in Figure 3(a). Figure 3(b), (c), (d) and (e) show the detailed backscatter electron micrograph of stratified microstructure. Qualitatively, an increase in concentration of Mo in the U-Mo terminal alloy has resulted in IDZs with less stratification (e.g., number of strata).

In order to determine the exact phase constituents of the IDZ in the U-Mo alloys vs. pure Al diffusion couples, TEM samples from selected regions within the IDZ were prepared. Figure 4 shows a summary of the phase distribution based on TEM analysis: UAl_4, UAl_3, $U_6Mo_4Al_{43}$, and UMo_2Al_{20} phases were identified in the IDZ. The phases labeled in black have been confirmed by SAED or CBED, while those marked in white have been estimated from the ternary phase diagram [31], results reported by others, and SEM/XEDS analyses of this study. At least two separate three-phase layers, or strata, were observed in the IDZ of this couple. Figures 5 and 6 show typical CBED and SAED patterns of the phases observed in the IDZ.

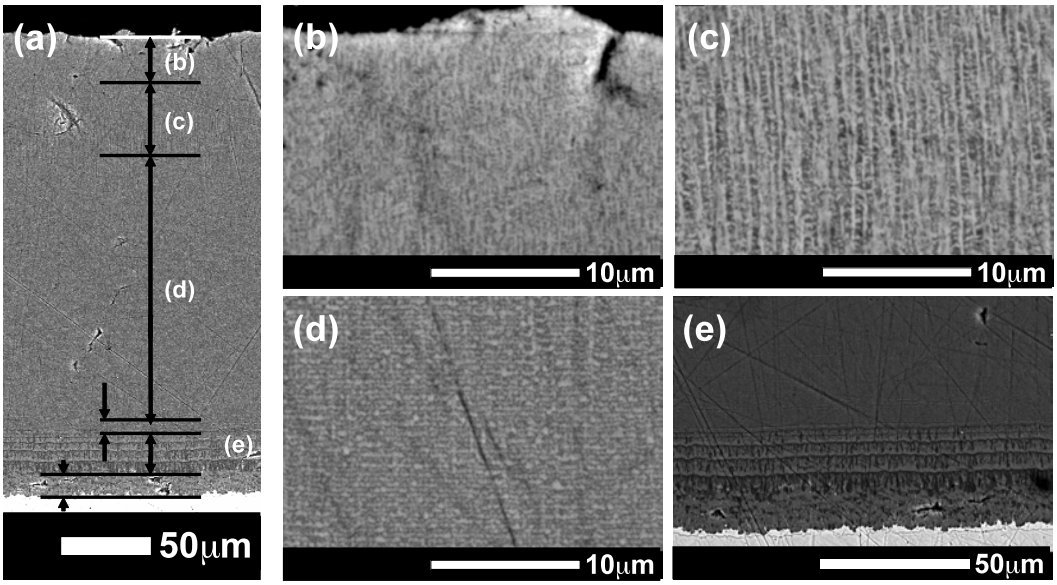

Figure 3. Backscatter electron micrographs of the IDZ in the U-7Mo vs. Al couple annealed at 600°C for 24 hours: (a) the complete IDZ; (b), (c), (d) and (e) show detailed regions within the IDZ.

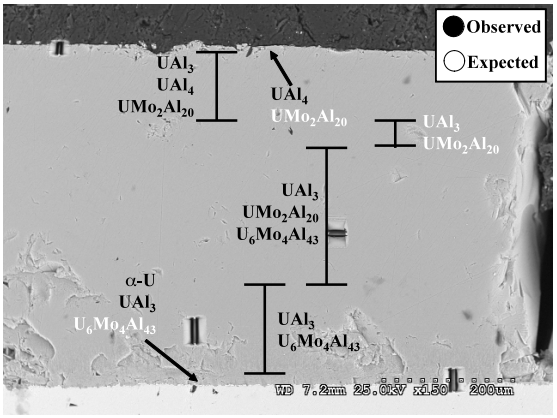

Figure 4. Summarized results from analytical TEM characterization of the IDZ developed in U-10Mo vs. Al diffusion couple annealed at 600°C for 24 hours. Those highlighted in black have been positively identified while those highlighted in white are estimated based on concept of diffusion path on the isothermal ternary diagram.

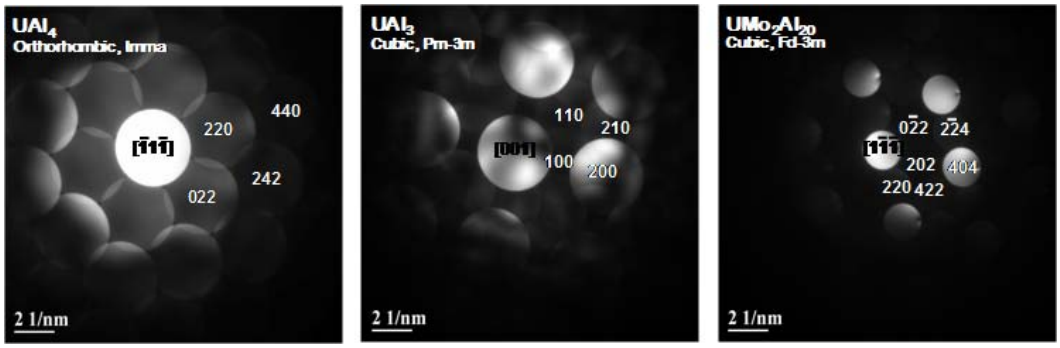

Figure 5. Typical CBED collected from UAl_4, UAl_3, UMo_2Al_{20} phases in the IDZ of the U-10Mo vs. Al diffusion couple annealed at 600C for 24 hours.

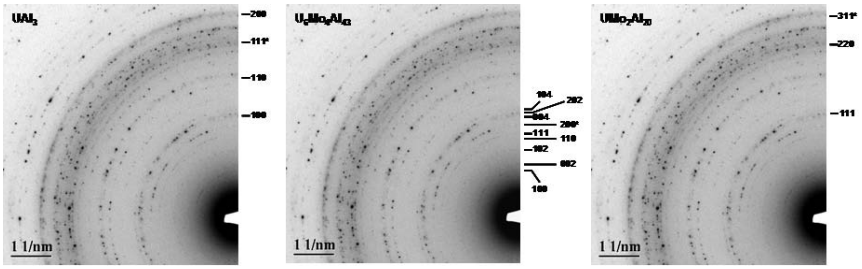

Figure 6. Electron diffraction patterns from the thick, center strata in the IDZ consisting of UAl_3, (b) $U_6Mo_4Al_{43}$ and (c) UMo_2Al_{20} phases.

Diffusion couples, U-7Mo, U-10Mo and U-12Mo vs. Al have been also annealed at 550°C for 1 hours. The time of diffusion anneal, reported in this paper, has been restricted to avoid any complication arising from the decomposition of U-Mo alloy. Table II reports the measured thickness of the IDZs, along with the growth constant. As expected the parabolic growth constant at 550°C decreased to 0.4~0.7 μm/sec$^{1/2}$ from 1~2 μm/sec$^{1/2}$determined at 600°C. Again, a maximum thickness was observed for U-10Mo vs. Al diffusion couple. The diffusion couples developed similar stratified microstructure within the IDZs to those observed after annealing at 600°C for 24 hours. The minimum stratification was observed for the U-12Mo vs. Al diffusion couple.

Table II. Thickness and diffusion-controlled growth constant for the interaction zones in diffusion couples of U-7Mo, U-10Mo and U-12Mo vs. Al annealed at 550°C for 1 hour.

Diffusion Couple	IDZ thickness (μm)	Growth Constant, K (μm/sec^{½})
U-7Mo vs. Al	31.4 ± 1.8	0.52
U-10Mo vs. Al	40.4 ± 0.6	0.67
U-12Mo vs. Al	22.4 ± 1.2	0.37

3.2 Diffusion couples U-Mo vs. Al-Si alloys

Diffusion couples consisting of U-7Mo, U-10Mo and U-12Mo vs. Al-2Si and Al-5Si were annealed at 550°C for up to 20 hours. This paper reports only the results from selected annealing time wherein no decomposition of the U-Mo alloys was observed. Those couples not reported in Table III (denoted by *) developed IDZ with highly non-planar interfaces (e.g., typical of interaction layer coupled with decomposition) and the thickness of the IDZ could not be measured within standard deviation of ±25%. However it should be noted that the decomposition of the γ(bcc) phase is strongly influenced by the absence/presence of Si, and subsequently couples with the growth of IDZs. Table III summarizes the thickness and growth constants, K, and reports that the assumed parabolic growth constant for U-Mo vs. Al-Si couples decreases to 0.1~0.2 μm/sec$^{1/2}$ from 0.4~0.7 μm/sec$^{1/2}$ determined for U-Mo vs. pure Al diffusion couples at 550°C.

SEM/XEDS analyses of selected diffusion couples showed that the stratified microstructure was better differentiated into two regions labeled (I) and (II) in Figure 7. XEDS maps from the IDZ show that there is a Si- and Al-rich stratum located near the U(Mo)/IDZ interface and IDZ/Al(Si) interface, respectively. The Si-rich layer can contain up to 70 at.% Si. The location of the Si- and Al-rich strata was observed to change as a function of Mo content in the U-Mo alloy. The Si-rich layer was observed within the IDZ near the IDZ/Al(Si) interface for U-7Mo vs. Al-Si diffusion couples, while it was located near the U(Mo)/IDZ interface for couples with U-10Mo and U-12Mo alloys.

Table III. Measured thickness and diffusion-controlled growth constant of the IDZ in selected diffusion couples, U-7Mo, U-10Mo and U-12Mo vs. Al-2Si annealed at 550°C up to 20 hours.

Diffusion Couple	1 hour Thickness (μm)	1 hour Growth Constant, K ($\mu m/sec^{1/2}$)	5 hours Thickness (μm)	5 hour Growth Constant, K ($\mu m/sec^{1/2}$)	20 hours Thickness (μm)	20 hour Growth Constant, K ($\mu m/sec^{1/2}$)
U-7Mo vs. Al-2Si	8.4 ± 1.4	0.14	*		*	
U-10Mo vs. Al-2Si	9.7 ± 3.4	0.16	22.2 ± 3.1	0.17	*	
U-12Mo vs. Al-2Si	10.1 ± 1.6	0.17	20.6 ± 2.3	0.15	52.2 ± 3.3	0.19
U-7Mo vs. Al-5Si	7.0 ± 1.3	0.12	11.9 ± 2.5	0.10	*	
U-10Mo vs. Al-5Si	8.6 ± 2.0	0.14	24.0 ± 1.8	0.18	56.7 ± 6.4	0.20
U-12Mo vs. Al-5Si	6.8 ± 0.7	0.11	12.1 ± 2.8	0.09	28.9 ± 1.9	0.11

* Not reported in this paper due to decomposition of the U-Mo alloy.

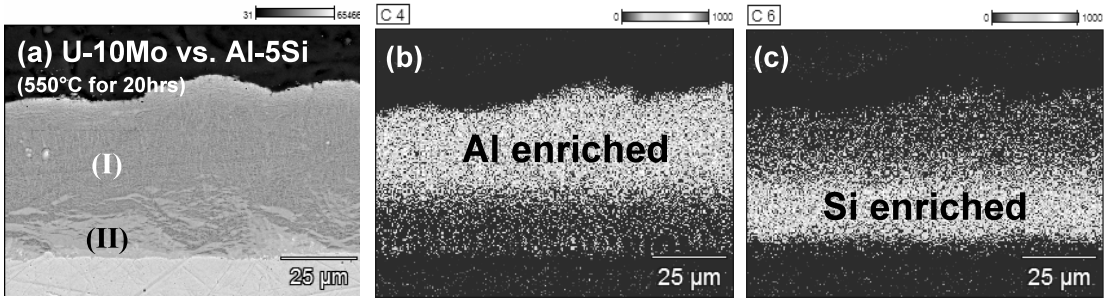

Figure 7. BE micrographs and XEDS maps of the U-10Mo vs. Al-5Si diffusion couple annealed at 550°C for 20 hours emphasizing the Al and Si distributions in the IDZ.

TEM analyses were carried out on the U-7Mo vs. Al-5Si diffusion couple annealed at 550°C for 5 hours. The TEM sample employed contained the entire thickness of the IDZ, and some of the U(Mo) and Al(Si) alloys as shown by a high angle annular dark field (HAADF) micrograph in Figure 8. Figure 8 clearly shows the three strata, labeled (I), (II) and (III). The SAED patterns from the IDZ, shown in Figure 9, revealed the main presence of $(U,Mo)(Al,Si)_3$ with UMo_2Al_{20} phases distributed throughout the IDZ. The $(U,Mo)(Al,Si)_3$ and UMo_2Al_{20} phases correspond to light gray matrix and dark gray spots, respectively, in HAADF image in Figure 8. *More importantly, with the presence of Si in the IDZs, the $U_6Mo_4Al_{43}$ and UAl_4 phases were not observed.*

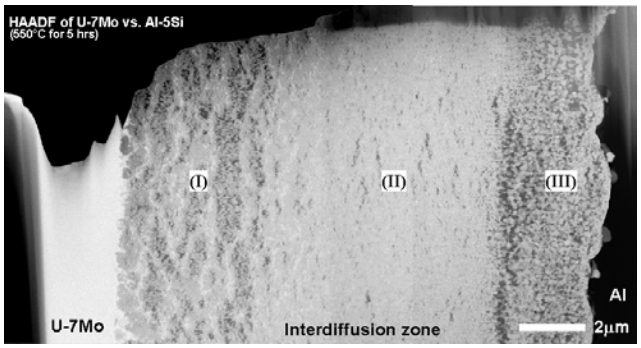

Figure 8. High angle annular dark field micrograph of the IDZ in the U-7Mo vs. Al-5Si diffusion couple annealed at 550°C for 5 hours.

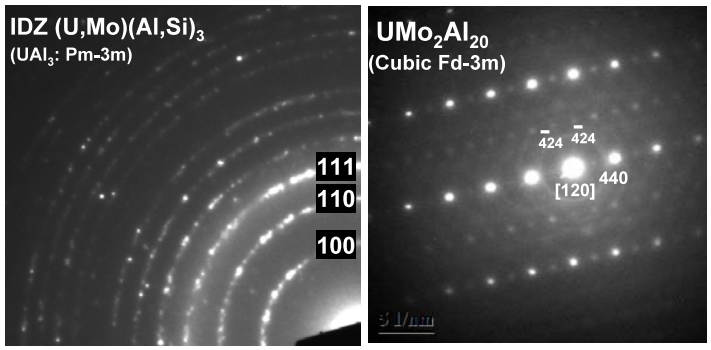

Figure 9. Typical SAED patterns demonstrating the presence of $(U,Mo)(Al,Si)_3$ and UMo_2Al_{20} phases within the IDZ of the U-7Mo vs. Al-5Si diffusion couple annealed at 550°C for 5 hours.

4. Discussion

In a parallel study [12,47] carried out to characterize the homogenized cast-alloys, 85.7Al-11.44U-2.86Mo and 87.5Al-10U-2.5Mo in at.%, whose compositions were chosen based on the typical average composition of the IDZ reported in literature [33,46,47], the UAl_4, UAl_3, $U_6Mo_4Al_{43}$ and UMo_2Al_{20} phases were observed to be the related phases for these compositions. Also in these cast-alloys, due to high Al content, the Al solid solution UAl_4 and UMo_2Al_{20} were determined as the equilibrium phases, not UAl_3. Thus, given the concentration profiles with negligible gradients, interdiffusion in U-Mo vs. pure Al couples may occur via supersaturated UAl_4 followed by "local-composition-dependent" equilibrium transformation involving UAl_4, UAl_3, $U_6Mo_4Al_{43}$, and UMo_2Al_{20} phases. This phenomena will require a specie that diffuses intrinsically much faster than other, *viz.*, Al.

Furthermore, in U-Mo vs. Al diffusion couple, several three-phase layers, were observed within the IDZ. Based on equilibrium thermodynamics (Gibbs' phase rule), three-phase layers cannot exist and grow in the IDZ for a ternary system with a constant temperature and pressure. Thus the analysis of interdiffusion in U-Mo vs. Al diffusion couples would require departure from a classical diffusion framework that assumes the local thermodynamic equilibrium.

The addition of Si resulted in reduced thickness of the IDZ by a factor of 3 to 4 defined by the growth constant. Based on the TEM analysis, the addition of Si appears to prevent the formation and development of the Al-rich UAl_4 and $U_6Mo_4Al_{43}$ phases within the IDZ. The Si addition appears to promote the formation of $(U,Mo)(Al,Si)_3$. Still, the Al-rich UMo_2Al_{20} phase was observed.

Disappearance of UAl_4 and $U_6Mo_4Al_{43}$ phases with Si addition may be attributed to the fact that USi_3 is the Si-richest phase in the U-Si system, and thermodynamically more stable than UAl_4. For example, the melting point of USi_3, UAl_3 and UAl_4 phases are 1510°, 1350° and 731°C, respectively. The location of the Si-rich layer, and correspondingly the Al-rich layer, would depend on the intrinsic diffusion of Si and Al in the presence of U and Mo. Change in location of Si-rich and Al-rich layers also suggests that the intrinsic diffusion coefficients of Si and Al are sensitive to the Mo (silicide-former) content in the U-Mo alloys. Presence of these Si- and Al-rich layers may also depend on total Si available, and thus time of diffusion anneal in the case of finite boundary conditions.

5. Conclusion

Interdiffusion and microstructural development in the U-Mo-Al system was examined using solid-to-solid diffusion couples consisting of U-7Mo, U-10Mo and U-12Mo vs. pure Al (wt.%), annealed at 600°C for 24 hours, and U-7Mo, U-10Mo and U-12Mo vs. pure Al, Al-2Si and Al-5Si (wt.%) annealed at 550°C for up to 20 hours. The UAl_4, UAl_3 $U_6Mo_4Al_{43}$ and UMo_2Al_{20} phases were observed to develop in high purity U-Mo vs. Al diffusion couples. The presence of negligible concentration gradient and three-phase regions in the interaction layer suggest a departure from local thermodynamic equilibrium. The introduction of Si into Al resulted in a significant reduction in the growth rate of IDZ. The $(U,Mo)(Al,Si)_3$, with large solubility for Mo and Si, and the UMo_2Al_{20} were the only phases observed to develop in these couples.

6. Acknowledgements

This work was financially supported by Idaho National Laboratory (Contract No. 00051953) under the operation of U.S. Department of Energy – Battelle Energy Alliance, LLC (DE-AC07-05ID14517). Additional financial support from CAREER Award of National Science Foundation (DMR-0238356) is gratefully acknowledged by the author, Yongho Sohn. Any opinions, findings, and conclusions or recommendations expressed in this manuscript are those of the authors and do not necessarily reflect the view of the National Science Foundation.

7. References

[1] D.D. Keiser Jr, S.L. Hayes, M.K. Meyer, C.R. Clark, JOM, (2003), 55.
[2] Federal Register, Vol. 51, No. 37, Feb. 25, 1986 / Rules and Regulations.
[3] M. Meyer, G.L. Hofman, S. Hayes, C. Clark, T. Wiencek, J. Snelgrove, R. Strain, K.H. Kim, J. Nucl. Mater., 304 (2002) 221.
[4] H.J. Ryu, Y.S. Han, J.M. Park, S. D. Park, C. K. Kim, J. Nucl. Mater. 321 (2003) 210.
[5] S.L. Hayes, M.K. Meyer, G.L. Hofman, Proceedings of the International Meeting on RERTR, Sao Paulo, Brazil, October 18-23, 1998.
[6] J. Snelgrove, G.L. Hofman, M.K. Meyer, C.L. Trybus, T.C. Wiencek, Nucl. Eng. Des. 178 (1997) 119.
[7] M.E. Kassner, P.H. Adler, M.G. Adamson, D.E. Peterson, J. Nucl. Mater., 167 (1989) 160.
[8] S. C. Parida, S. Dash, Z. Singh, R. Prasad, V. Venugopa, J. Phys. Chem. Solids, 62 (2001), 585.
[9] F. Muhammad, A. Majid, Prog. Nucl. Engy. (2008) 1-8.
[10] F. Muhammad, A. Majid, Annals Nucl. Energy, 36 (2009), 998.
[11] K.H. Kim, D.B. Lee, C.K. Kim, G.E. Hofman, K.W. Paik, J. Nucl. Mater., 245 (1997), 179.
[12] E. Perez, A. Ewh, J. Liu, B. Yuan, D.D. Keiser Jr., Y.H. Sohn, J. Nucl. Mater., (2009) in press.
[13] D.B. Lee, K.H. Kim, C. K. Kim, J. Nucl. Mater., 250 (1997) 79.
[14] G.L. Hofman, M.K. Meyer, Y-M Park, Proceedings of the International Meeting on RERTR, Las Vegas NV, October 1-6, 2000.
[15] N. Wieschalla, A. Bergmaier, P. Böni, K. Böning, G. Dollinger, R. Großmann, W. Petry, A. Röhrmoser and J. Schneider, J. Nucl. Mater., 357 (2006) 191.
[16] K.H. Kim, J.M. Park, C.K. Kim, G. L. Hofman and M. K. Meyer, Nucl. Eng. Design, 211 (2002) 229.

[17] A. Leenaers, S. Van den Berghe, E. Koonen, C. Jarousse, F. Huet, M. Trotabas, M. Boyard, S. Guillot, L. Sannen, M. Verwerft, J. Nucl. Mater., 335 (2004) 39.
[18] E. Perez, N. Hotaling, A. Ewh, D.D. Keiser, Y.H. Sohn, Def. Diff. For., 266 (2007) 149.
[19] F. Muhammad, A. Majid, Annals Nucl. Energy, 35 (2008) 1720-1731.
[20] H. Noël, O. Tougait, S. Dubois, J. Nucl. Mater., 389 (2009) 93-97.
[21] S.H. Lee, J.C. Kim, J.M. Park, C.K. Kim, S.W. Kim, Int. J. Thermophys., 24 (2003) 1355.
[22] D. Olander, J. Nucl. Mater., 383 (2009), 201.
[23] J.M. Park, H.J. Ryu, S.J. Oh, D.B. Lee, C.K. Kim, Y.S. Kim, G.L. Hofman, J. Nucl. Mater., 374, (2008), 422.
[24] H.J. Ryu, J.M. Park, C.K. Kim, Y.S. Kim, G.L. Hofman, J. Phase Equil. Diff., 27 (2006) 651.
[25] M.I. Mirandou, S.F. Aricó, S.N. Balart, L.M. Gribaudo, Mater. Char., 60 (2009) 888.
[26] M.I. Mirandou, S.F. Aricó, M. Rosenbusch, M. Ortiz, S. Balart, L. Gribaudo, J. Nucl. Mater., 384 (2009) 268.
[27] K.H. Kim, D.B. Lee, C.K. Kim, G.E. Hofman, K.W. Paik, J. Phys. Chem. Solids, 62 (2001) 585.
[28] H.J. Ryu, Y.S. Kim, G.L. Hofman, J.M. Park, C.K Kim, J. Nucl. Mater., 358 (2006) 52.
[29] R. Ahmed, Aslam, N. Ahmad, Annals Nucl. Energy, 32 (2005) 29.
[30] R. Ahmed, Aslam, N. Ahmad, Annals Nucl. Energy, 32 (2005) 1100.
[31] S.H. Lee, J.C. Kim, J.M. Park, C.K. Kim, S.W. Kim, Int. J. Thermophysics, 24, No. 5, (2003) 1355.
[32] D.D. Keiser Jr., Def. Diff. For., 266 (2007) 131.
[33] C.K. Varela, M. Mirandou, S. Aricó, S. Balart, L. Gribaudo, Proceedings of the RRFM and IGORR, Centre de Congrès, Lyon, France March 11-15, 2007, 135.
[34] M.I. Mirandou, S.N. Balart, M. Ortiz, M.S. Granovsky, J. Nucl. Mater., 323 (2003) 29.
[35] D. Subramanyam, M.R. Notis, J. I. Goldstein, Metall. Trans. A, 16A (1985) 589.
[36] T.K. Bierlein, D.R. Green, Nucl. Sci. Eng., 2 (1957) 778.
[37] Mazaudier, C. Proye, F. Hodaj, J. Nucl. Mater., 377 (2008) 476
[38] S.Van den Berghe, W.Van Renterghem, A. Leenaers, J. Nucl. Mater., 375 (2008) 340.
[39] H.J. Ryu, Y.S. Kim, G.L. Hofman, J. Nucl. Mater., 385 (2009), 623.
[40] D.D. Keiser, A.B. Robinson, J.F. Jue, P. Medvedev, M.R. Finlay, Proceedings of the RRFM, Vienna Int. Ctr., Vienna, Austria, March, 22-25, 2009.
[41] Y.H. Sohn, N. Garimella, E. Perez, R. Mohanty, J. Liu, Def. Diff. For., 258 (2006) 346
[42] E. Perez, D.D. Keiser, Y.H. Sohn, Def. Diff. For.,, 289 (2009) 41.
[43] S.H. Lee, J.M. Park, C.K. Kim, Int. Jour. Thermophysics, 28 (2007) 1578.
[44] P.E. Repas, R.H. Goodenow, R.F. Hehemann, Trans. ASM, 57 (1964) 150.
[45] H. Palancher, P. Martin, V. Nassif, R. Tucoulou, O. Proux, J.-L. Hazemann, O. Tougait, E. Lahéra, F. Mazaudier, C. Valot, S. Dubois; J. Appl. Cryst. 40 (2007) 1064.
[46] F. Mazaudier, C. Proye, F. Hodaj; Proceedings of the RRFM, Sofia, Bulgaria, April, 30 – May 3, 2006, 87.
[47] D.D. Keiser Jr., C.R. Clark, M.K. Meyer, Scr. Mater. 51 (2004) 893.
[48] H. Palancher, N. Wieschalla, P. Martin, R. Tucoulou, C. Sabathier, W. Petry, J.F. Berar, C. Valot, S. Dubois, J. Nucl. Mater. (2009) in Press.